Progress In Electromagnetics Research, Vol. 163, 79–87, 2018

Design of Two Ku-Band Orthomode Transducers for Radio Astronomy Applications

Renzo Nesti[1], Elia Orsi[2], Giuseppe Pelosi[2], and Stefano Selleri[2, *]

Abstract—Two different designs of orthomode transducers for the coming Ku-band receiver of the Italian radio telescope in Medicina are presented and compared, showing design details, describing numerical simulations and discussing manufacturing and test results. Such orthomode transducers provide a tradeoff between low-loss and phase-matching, according to different initial requirements where the final receiver architecture has to be frozen. Both designs show high performance over the operative 13.5–18.1 GHz Ku-band. One of the OMT designs has been fabricated and tested, showing results in very good agreement with simulations.

1. INTRODUCTION

Orthomode transducers (OMTs) are passive and reciprocal microwave components able to separate two orthogonal linear polarizations impinging at its input port into two separate channels. Due to this, OMTs are commonly used in telecommunication front-end receivers to reuse frequencies or, with a differential phase shifter, (DPSs) [1] to form polarizers [2], which allows to separate an input signal into its right and left hand circular polarization components.

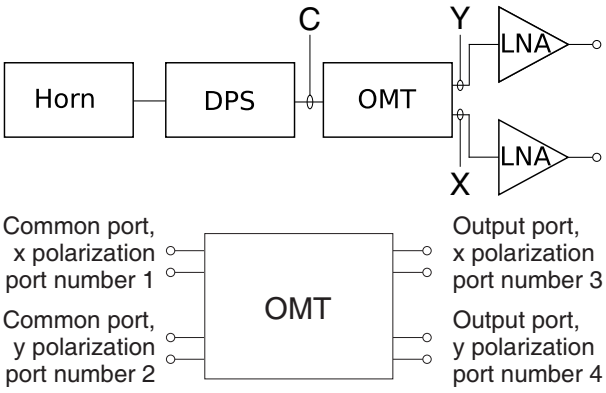

Figure 1. Top: Block diagram of a receiver front-end with polarization separation. The common (C) port of the OMT as well as the two output port yielding Y and X polarizations are also highlighted. Bottom: Electrical port numbering scheme for the OMT.

This latter device is also used to study the state of polarization of the input electromagnetic wave in radio telescopes. In this case, the receiving chain is shown in Fig. 1, with the horn in the focus of

Received 20 June 2018, Accepted 31 August 2018, Scheduled 12 September 2018
* Corresponding author: Stefano Selleri (stefano.selleri@unifi.it).
[1] Italian National Institute for Astrophysics (INAF), Arcetri Astrophysical Observatory, Florence I-50125, Italy. [2] Department of Information Engineering (DINFO), University of Florence, Via di S. Marta, 3, Florence I-50139, Italy.

the radio telescope optics, followed by the DPS and the OMT and finally by the low noise amplifiers (LNAs), the complete system possibly being cryogenically cooled to enhance its noise figure. Due to the extremely faint signal to detect in radio astronomy, low loss and very high polarization separation capabilities over broad bandwidths are a must.

The performance of OMTs highly depends on the device's geometrical and electrical symmetry, and therefore, they can be classified according to this parameter, as it has been firstly made by Bøifot et al. in [3], where three classes are defined: class one [4] holds the simplest OMT to be fabricated, consisting of one main arm and a single side arm, each of which allows only one polarization. Class two [5, 6] holds somewhat more symmetric and complex OMTs: the side arm splits into two branches which are symmetric with respect to the main arm. Finally, class three [7] includes the most symmetrical OMTs, like the ones based on a turnstile junction [8]. The OMTs presented in this paper fall in the last category.

Actually, another classification exists, [9, 10], based on the type of waveguides and discontinuities in the OMT. Such a classification comprises, for example, septum, dual-junction, microstrip coupled and coaxial coupled OMTs.

In this paper the electromagnetic design of two different OMTs is presented. The devices are designed for a Ku-band receiver for the radio telescope located in Medicina (Bologna, Italy) and operated by the Italian National Institute for Astrophysics (INAF). For easy machining, assembly, and in order to have low-cost production, both designs are thought for exploiting platelet fabrication technique, which has already been tested for radio astronomical applications [11].

The paper is organized as follows. Section 2 presents the OMTs design. Section 3 discusses the design robustness, with a comparison between measurements and numerical simulations, also taking into account tolerance analysis. Finally Section 4 draws some conclusions.

2. DESIGN

The electromagnetic requirements for this application are: $|S_{ii}| < -20\,\text{dB}$, loss less than 0.2 dB, over the 13.5–18.1 GHz band, which are quite demanding, especially for what concerns bandwidth. Two designs have been devised to meet these requirements, both based on the same turnstile junction [8] and two pairs of waveguide arms joining at the two output ports: a hybrid one (Fig. 2) and an equalized one (Fig. 3). In both designs the input port is a circular waveguide with radius 8.05 mm, and the two output ports are in WR62.

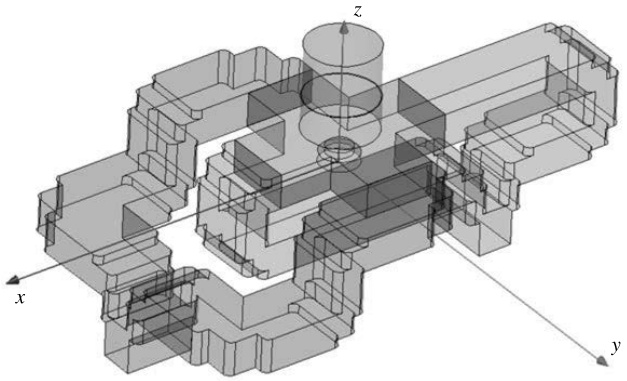

Figure 2. Hybrid OMT's design.

All designs have been firstly simulated via a Finite Elements Methods (FEM) based commercial software (HFSS) exploiting adaptive meshing up to about three thousands tetrahedral cells per unit wavelength cube volume. Ports are waveguide type, two rectangular, in single mode operation, and one is circular, with two orthogonal TE_{11} modes. Even if each port operates in its unimodal band, waveguide port fields are expanded exploiting 3 higher order modes for a more accurate field expansion. The boundaries other than the ports have been modeled with a finite conductivity surface boundary

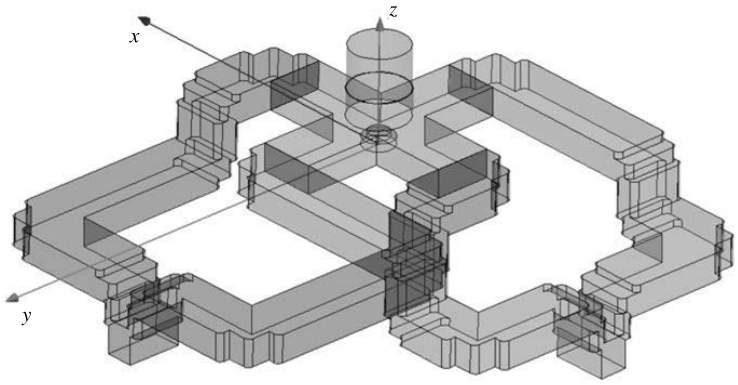

Figure 3. Equalized OMT's design.

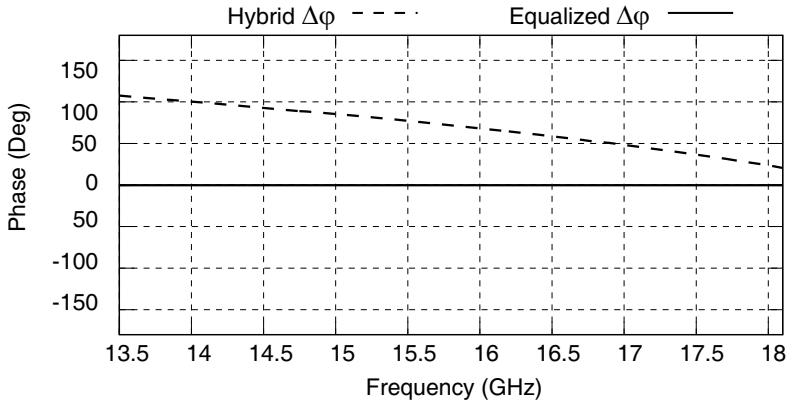

Figure 4. Differential phase shift between the two polarizations of both models.

condition, able to analytically include also surface roughness characteristics. All these considered, simulations accuracy is expected to be within 1% of the real value.

About the two models, the hybrid model is optimized for compactness so as to minimize loss, but it has different recombining paths, and thus it does not exhibit phase matching between them. The equalized model exhibits longer paths than the hybrid, and thus higher loss, but the two recombining branches have the same physical (and electrical) length, hence the associated transmission coefficient phase delays are equal. Fig. 4 shows the simulated differential phase shift $\Delta\phi$ between each pair of polarization paths of the two designs, with almost perfect phase matching for the equalized design.

Phase equalization preserves the polarization information of the input signal at hardware level, allowing in principle to fully reconstruct its state easily and directly. For the hybrid model polarization reconstruction would require more devices and sophisticated calibration procedures.

It is important to point out that, in contrast to what one might think, the hybrid model is more symmetric than the equalized one. Indeed, the former has one plane of symmetry, that is the xz plane (Fig. 2), while the latter does not have any plane of symmetry and hence will exhibit worse crosstalk characteristics, as shown in the following.

Regarding the input matching of the turnstile junction, very good performance has been achieved using two cylinders (Fig. 5) which keep the structure's symmetry [12], but square [13] or other geometries [14] or a third or fourth cylinder in the turnstile junction [15] can also be adopted. The convenient choice among alternative geometries mainly depends upon mechanical manufacturing process.

Although the OMT performance versus bandwidth of the proposed design is basically equivalent to those given in most of recently published waveguide-based OMT papers, the architecture used in this paper for both OMTs adds unique features compared to them, features which are mandatory in this

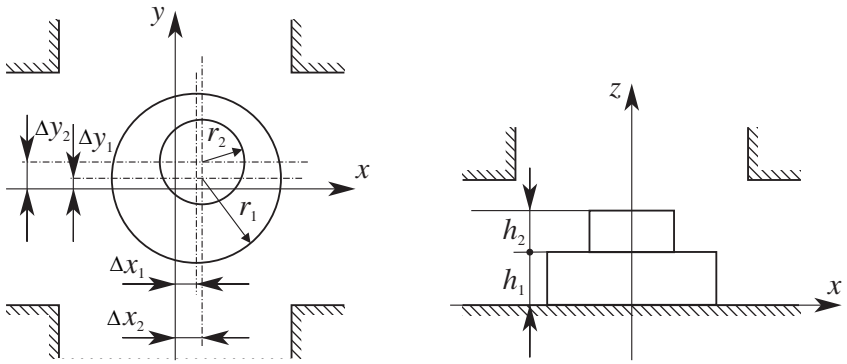

Figure 5. Geometry of the turnstile junction, with highlighted both the disk dimensions and the possible tolerances in disk placement, nominal (x, y) position of disk centers being $(0, 0)$.

particular application. With respect to OMT based on the Bøifot junction [3] one important advantage is to have a circular waveguide common port that can be directly connected to the circular horn as in this case; another important advantage with respect to recently published papers on Bøifot junction derived OMTs, as for example [16] and [17], is the intrinsic symmetry in the waveguide recombination paths, that is best suited to have both amplitude and phase matching (as in the equalized model), and better compactness needs to be under the aperture feed shadow if the rectangular waveguide outputs need to be both in the backward direction and the overall OMT footprint.

By comparing the proposed OMTs to other recently published turnstile junction based OMTs [13], oriented to compactness and with excellent performance, it can be noticed that the solution proposed here leads to full platelet fabrication, different for example from [14], and the optimized geometry leads to a very limited number of layers, five in this case, about half with respect to, for example [18].

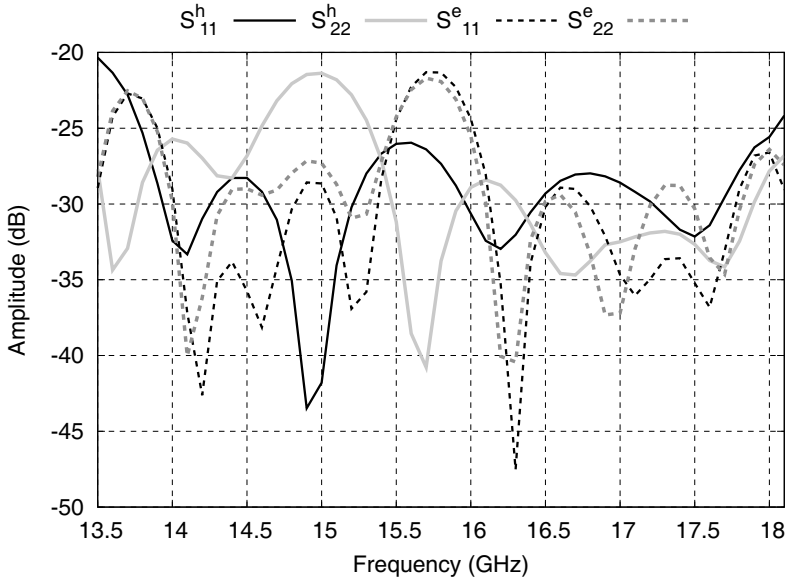

Figure 6. Comparison between reflection coefficients of the two OMTs for both polarizations. S^h_{ij} for hybrid model and S^e_{ij} for equalized model.

3. SIMULATIONS AND MEASUREMENTS

A comparison between the simulated reflection coefficients of the hybrid and equalized models is shown in Fig. 6, where electrical ports 1 and 2 correspond to the two polarizations of the single circular waveguide physical port. Differences between the two models are due to the differences in the recombining arms paths. Transmission coefficients are shown in Figs 7 and 8, where the surface-roughness ρ and the electrical-conductivity of the waveguide-wall σ are considered as parameters. Taking into account the instrumental accuracy and drifts, leading to an error of about 0.02 dB in the loss measurements, by comparing measurements vs simulations in Fig. 8, we can estimate the aluminum material used for

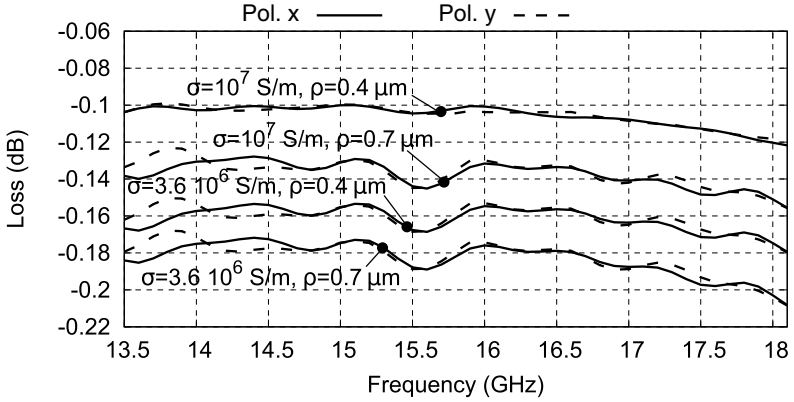

Figure 7. Equalized model simulated loss.

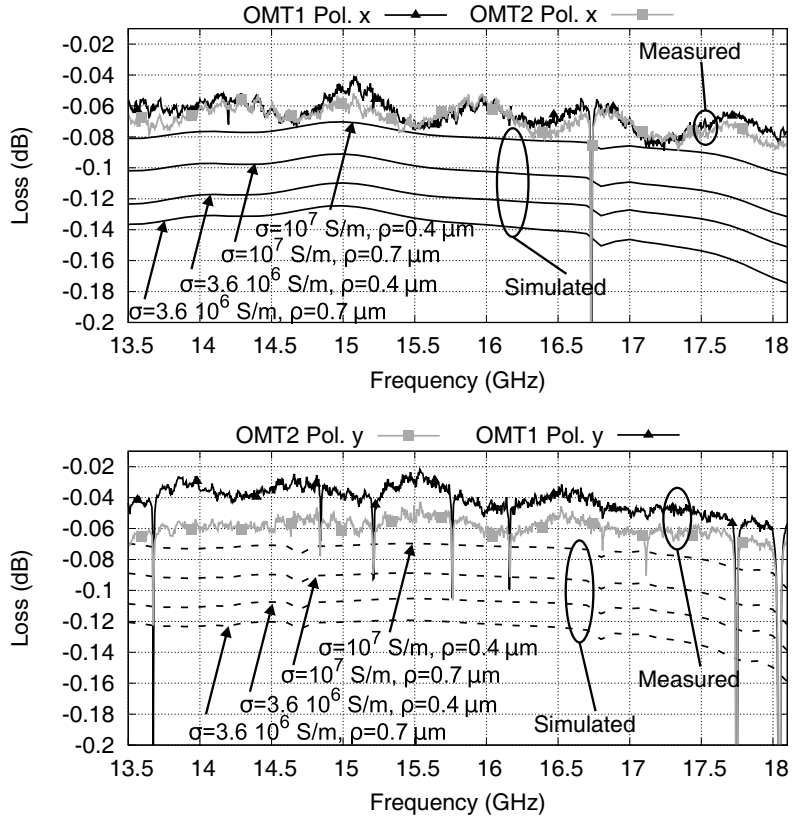

Figure 8. Hybrid model simulated and measured loss: top, x-polarization, bottom y-polarization.

prototyping a conductivity of about 10^7 S/m and a roughness of about 400 nm in very good agreement to what expected. The equalized model shows both phase and loss equalization between the two polarization channels, while the hybrid model exhibits different phase delays and losses in the two arms.

Since mechanical tolerances of both the waveguide paths and matching cylinders in the turnstile junction are very critical, they have been carefully optimized to match requirements, and a sensitivity analysis has been performed using values ranged in Table 1.

Table 1. Geometrical variation ranges.

Variation on the adapting disk geometry			
Δr_1 (mm)	Δh_1 (mm)	Δr_2 (mm)	Δh_2 (mm)
± 0.02	± 0.02	± 0.02	± 0.01

Variation on the adapting disk position			
Δx_1 (mm)	Δy_1 (mm)	Δx_2 (mm)	Δy_2 (mm)
± 0.02	± 0.02	± 0.02	± 0.02

Variation on the combiner-branch path-length
Δl (mm)
± 0.04

Although both designs are within the specifications, lower loss, and hence lower noise, were considered more relevant than phase matching, so the hybrid model has been chosen for prototyping (Fig. 9). Tolerance analysis results are thus shown only for this model, those related to the equalized model being very similar, where comparable. As regards phase matching tolerance analysis, which does not have sense in the hybrid model, errors within $\pm 0.4^\circ$ came out for the equalized model.

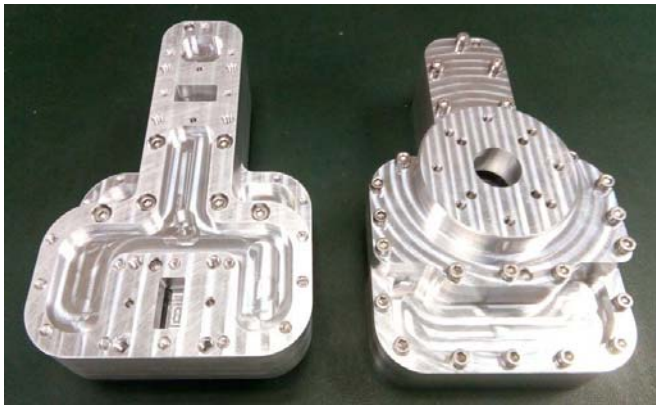

Figure 9. OMT platelet prototypes.
skip0.1in

Platelet technique has been chosen as fabrication process, and two prototypes, composed by five layers (including top and bottom flanges), with $133 \times 86 \times 53\,\text{mm}^3$ of envelope and 0.7 kg of weight were manufactured (Fig. 9).

Prototypes have been measured (Fig. 10) in a VNA setup environment using TRL (Thru-Reflect-Line) calibration procedure with custom-made optimized adapters connecting coaxial, rectangular and circular waveguides.

In Figs. 11 and 12 the results of the sensitivity analysis, in terms of reflection coefficient, are given as average (line) plus standard deviation (error bars) and compared to the hybrid model measurements,

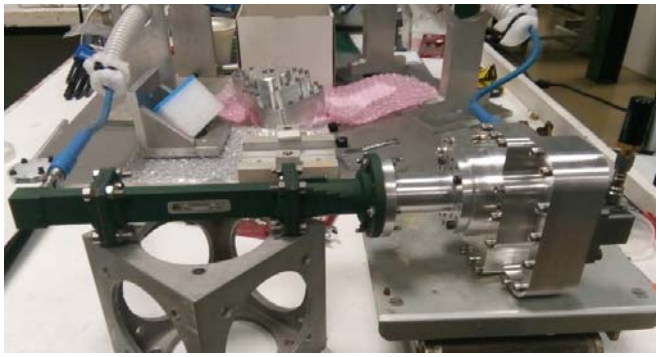

Figure 10. OMT measurement setup.

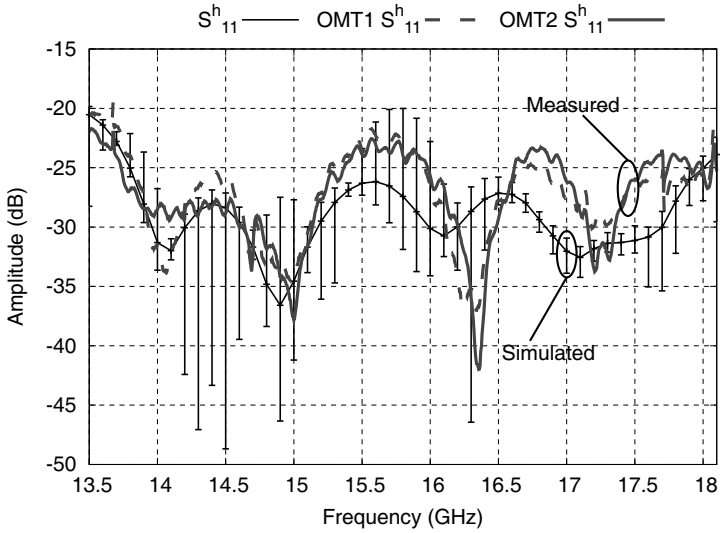

Figure 11. Hybrid model x-polarization measurements on prototypes and numerically predicted sensitivity to fabrication tolerances (average + standard deviation bars) on input matching.

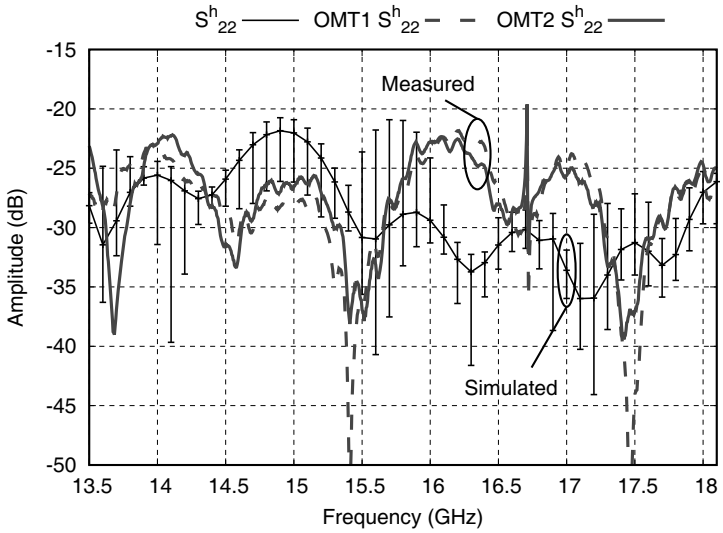

Figure 12. Hybrid model y-polarization measurements on prototypes and numerically predicted sensitivity to fabrication tolerances (average + standard deviation bars) on input matching.

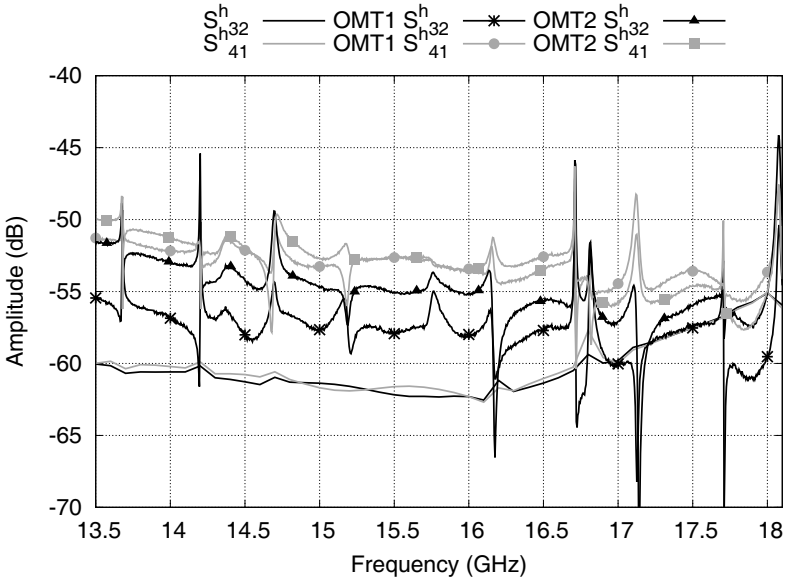

Figure 13. Hybrid model measurements and worst-case numerical analysis on fabrication tolerances due to crosstalk, the latter represented as the envelope of the transmission among uncoupled port pairs for different values of the geometrical tolerance.

showing very good agreement. Furthermore, the hybrid model fabrication process highlights a satisfying degree of reproducibility since the curves for the two prototypes are almost identical.

Crosstalk is another very important figure of merit, mainly originated by asymmetries due to fabrication tolerances and leading to undesired coupling between the x-polarization input port 1 and y-polarization output port 4 and between the y-polarization input port 2 and x-polarization output port 3. Results of crosstalk sensitivity analysis are given in the S_{32} and S_{41} curves of Fig. 13, together with measurements. The cross-talk level is excellent, even if quite sensitive to mechanical tolerances and test setup misalignments, as it can be seen in the difference between measured curves, remaining below -50 dB all over the bandwidth, also in the measurement data (except some trapped mode spikes). It is worth to point out that the more symmetric nature of the hybrid design leads to about 5 dB better crosstalk with respect to the equalized model (here not shown).

4. CONCLUSION

Two different designs of Ku-band orthomode transducers have been discussed and compared. Simulated results show the excellent behavior of both models in the operative frequency range (13.5–18.1 GHz) with reflection coefficient below -20 dB, loss better than 0.2 dB and crosstalk below -50 dB. Sensitivity analysis has also been presented highlighting the robustness of the OMT design to the mechanical tolerance of the order of 10 to 20 µm, typical of platelet fabrication. EM tests on two manufactured hybrid OMTs are in very good agreements with the expected performance and sensitivity analysis.

REFERENCES

1. Leal-Sevillano, C. A., J. R. Montejo-Garai, J. M. Rebollar, and J. A. Ruiz-Cruz, "CAD for dual-band polarizers in corrugated rectangular waveguide," *41st European Microwave Conference (EuMC)*, 822–825, Manchester, UK, Oct. 9–14, 2011.
2. Chang, C., S. Church, S. Tantawi, P. Larkoski, M. Sieth, and K. Devaraj, "Theory and experiment of a compact waveguide dual circular polarizer," *Progress In Electromagnetics Research*, Vol. 131, 211–225, 2012.

3. Bøifot, A. M., E. Lier, and T. Schaug-Pettersen, "Simple and broadband orthomode transducer (antenna feed)," *IEE Proc. H*, Vol. 137, 396–400, Dec. 1990.
4. Tiwari, V. N. and T. Tiwari, "Design and development of orthomode transducer for X-band frequency," *2015 IEEE Applied Electromagnetics Conference (AEMC)*, 1–2, Dec. 2015.
5. Ruiz-Cruz, J. A., J. R. Montejo-Garai, C. A. Leal-Sevillano, and J. M. Rebollar, "Development of folded dual-polarization dividers for broadband ortho-mode transducers," *Asia-Pacific Microwave Conference (APMC)*, Vol. 2, 1–3, Melbourne, AU, Dec. 5–8, 2015.
6. Banham, R., L. Lucci, V. Natale, R. Nesti, G. Pelosi, S. Selleri, G. Tofani, and G. Valsecchi, "Electroformed front-end at 100 GHz for radio-astronomical applications," *Microwave J.*, Vol. 48, No. 8, 112–122, 2005.
7. Park, S. G., H. Lee, and Y. H. Kim, "A turnstile junction waveguide orthomode transducer for the simultaneous dual polarization radar," *Asia-Pacific Microwave Conference (APMC)*, 135–138, Singapore, Dec. 7–10, 2009.
8. Meyer, M. A. and H. B. Goldberg, "Applications of the turnstile junction," *IRE Trans. Microw. Theory Tech.*, Vol. 3, No. 6, 40–45, 1955.
9. Gentili, G. G., R. Nesti, G. Pelosi, and S. Selleri, "Orthomode transducers," *The Wiley Encyclopedia of RF and Microwave Engineering*, K. Chang, Ed., Vol. 4, 3547–3563, John Wiley & Sons, New York, NY, 2005.
10. Uher, U. R. J. and J. Bornemann, *Waveguide Components for Antenna Feed Systems: Theory and CAD*, Artech House, Norwood, MA, 1993.
11. Lucci, L., R. Nesti, G. Pelosi, and S. Selleri, "A stackable constant-width corrugated horn design for high-performance and low-cost feed arrays at millimeter wavelengths," *IEEE Antennas Wireless Propag. Lett.*, Vol. 11, 1162–1165, 2012.
12. Chang, C., S. G. Tantawi, S. Church, J. Neilson, and P. V. Larkoski, "Novel compact waveguide dual circular polarizer," *Progress In Electromagnetics Research*, Vol. 136, 1–16, 2013.
13. Navarrini, A. and R. L. Plambeck, "A turnstile junction waveguide orthomode transducer," *IEEE Trans. Microw. Theory Tech.*, Vol. 54, 272–277, January 2006.
14. Srikanth, S. and M. Solatka, "A compact full waveguide band turnstile junction orthomode transducer," *XXXth URSI General Assembly and Scientific Symposium*, 1–4, Istanbul, TR, Aug. 13–20, 2011.
15. San-Blas, A.-A., F. Perez, J. Gil, F. Mira, V. Boria, and B. Gimeno Martinez, "Full-wave analysis and design of broadband turnstile junctions," *Progress In Electromagnetics Research Letters*, Vol. 24, 149–158, 2011.
16. Navarrini, A. and R. Nesti, "Symmetric reverse-coupling waveguide orthomode transducer for the 3-mm band," *IEEE Trans. Microw. Theory Tech.*, Vol. 57, No. 1, 80–88, 2009.
17. Ruiz-Cruz, J. A., J. R. Montejo-Garai, J. M. Leal-Sevillano, and C. A. Rebollar, "Orthomode transducers with folded double-symmetry junctions for broadband and compact antenna feed," *IEEE Trans. Antennas Propag.*, Vol. 66, No. 3, 1160–1168, 2018.
18. Virone, G., O. A. Peverini, M. Lumia, G. Addamo, and R. Tascone, "Platelet orthomode transducer for Q-band correlation polarimeter clusters," *IEEE Trans. Antennas Propag.*, Vol. 62, No. 7, 1487–1494, 2014.